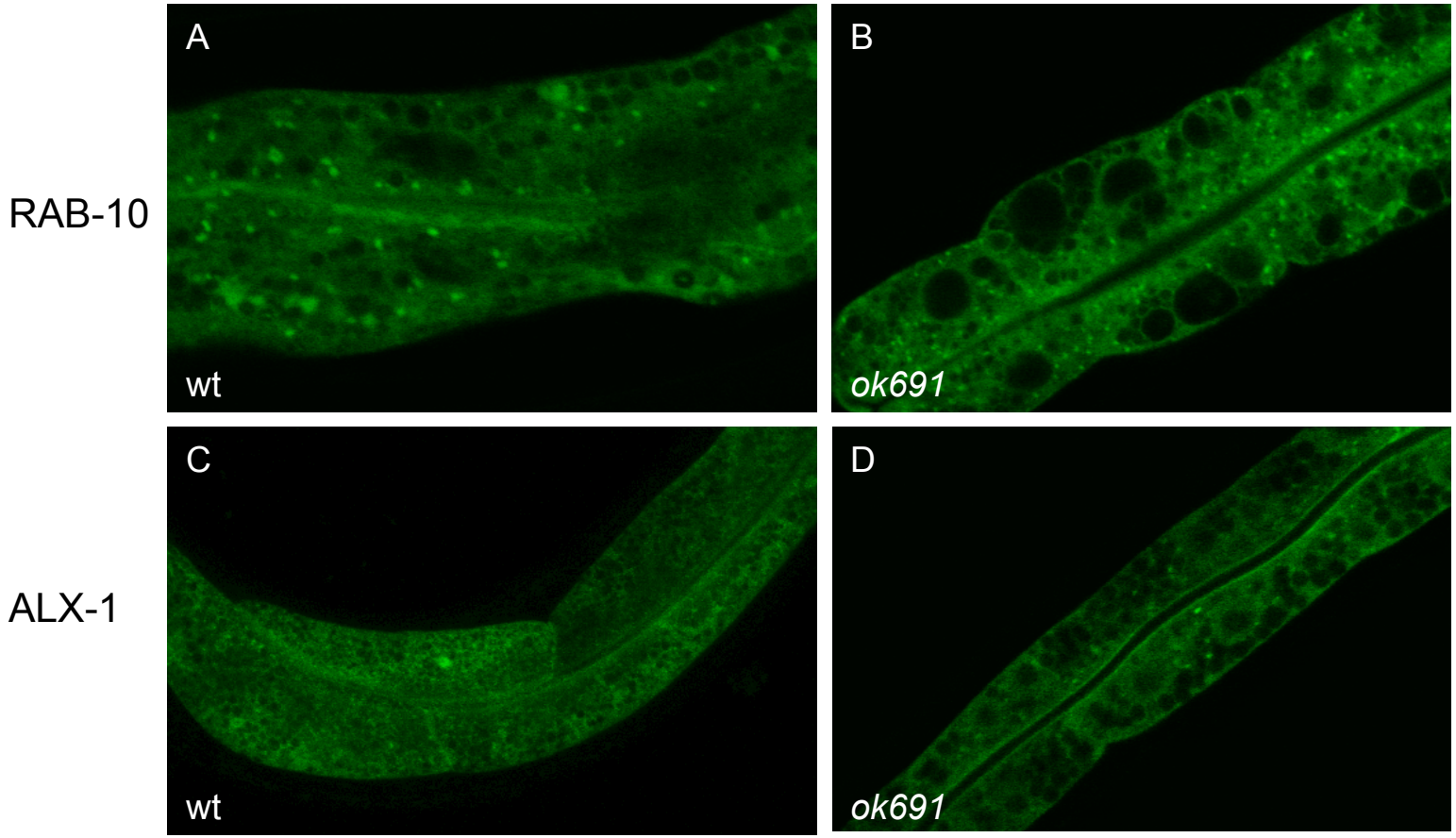

Fig. 1S: Morphology of recycling endosomes is not affected in *bec-1* mutants. Confocal images of GFP::RAB-10 in wild-type (A) and *bec-1* animals (B), and GFP::ALX-1 in wild-type (C), and *bec-1* mutant animals (D). GFP::RAB-10 is normally localized to early endosomes and Golgi in the intestine (Chen et al., 2006) of wild-type animals (A). In *bec-1 (ok691)* mutant animals GFP::RAB-10 does not label the enlarged endosomes and the GFP::RAB-10 expression and localization is similar to that of wild-type animals (B). GFP::ALX-1 is associated with recycling endosomes and multivesicular bodies, and promotes the recycling of basolateral cargo internalized independently of clatrhrin (Shi et al., 2007). In wild-type animals (C), GFP::ALX-1 is observed in small puncta in the basolateral region of the intestine. Although the puncta may appear slightly larger in *bec-1* mutant intestines (D), GFP::ALX-1 did not label the enlarged endosomes an the number of GFP::ALX-1 endosomes appeared similar to that of wild-type animals (C).

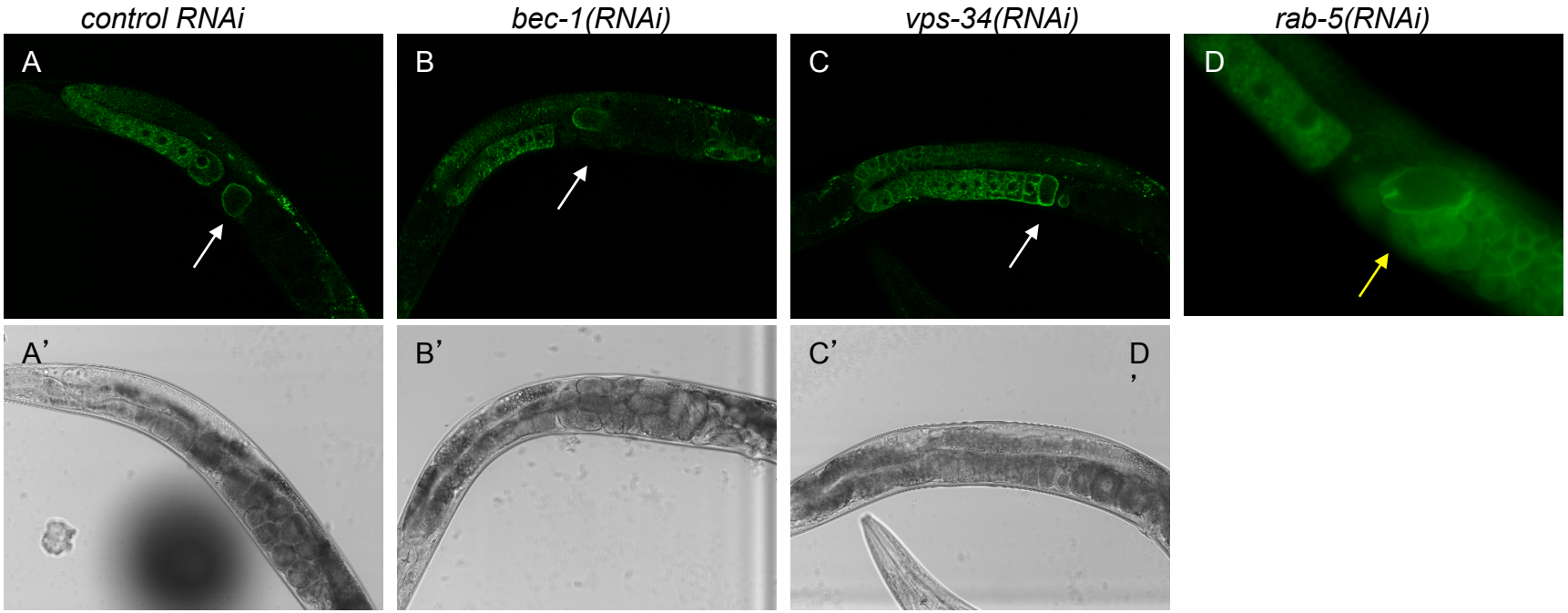

Fig. 2S: Degradation of CAV-1-GFP occurs in *bec-1* mutants. Localization of CAV-1::GFP was determined in *bec-1 (RNAi)* (C) and *vps-34(RNAi)* (D) animals by confocal microscopy. CAV-1::GFP is normally degraded via clathrin and RAB-5-dependent endocytosis after fertilization (K. Sato et al., 2006).The degradation of CAV-1::GFP appeared normal in *bec-1 (RNAi),* and *vps-34(RNAi)* treated animals, when compared to that of mock treated animals fed bacteria harboring the control empty RNAi vector (A and B). For each confocal CAV-1::GFP image (except *rab-5(RNAi)* animals) the Nomarski image is provided below (A' for mock L4440 RNAi treated, B' for *bec-1(RNAi)* and C' for *vps-34(RNAi)* treated animals. Other phenotypes associated with the knockdown of *bec-1* and *vps-34* function were observed (data not shown). We observed the lack of degradation in fertilized embryos of *rab-5* RNAi animals, an experiment performed in parallel (D). Magnification for images A-C is 200X, and for D, is 400X.

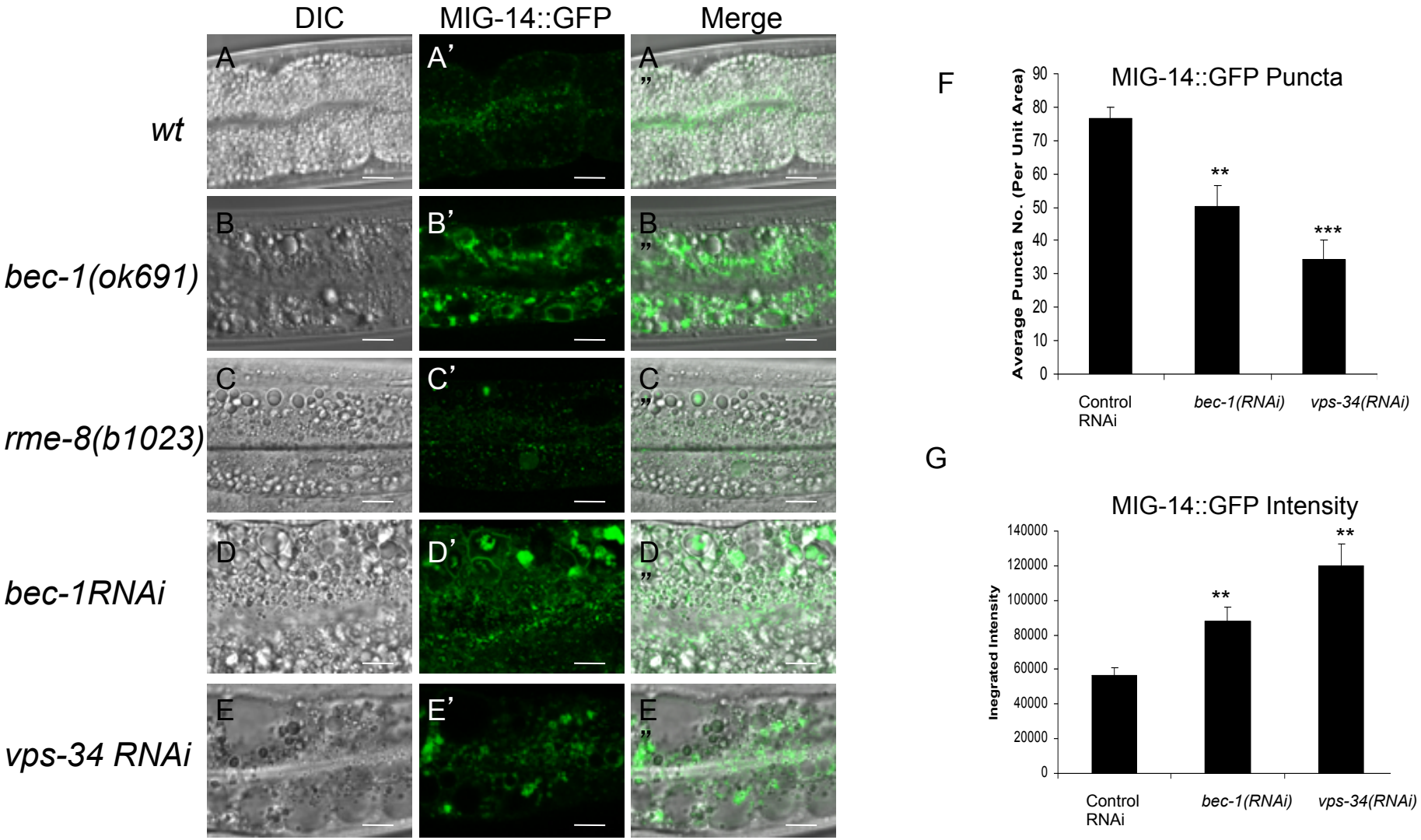

Fig. 3S: Lack of *bec-1* and *vps-34* affect the localization of MIG-14::GFP. Representative images of the expression of the retromer cargo protein MIG-14::GFP in wild-type animals (A,A', A"), *bec-1(ok691*) mutants (B,B', B"), *rme-8(b1023)* mutants (C,C' C"), and animals that have been treated with RNAi against *bec-1* (D,D', D") and *vps-34* (E,E,' E"). Left panels show the DIC Nomarski images, center panels show the MIG-14::GFP, and the right panels show the merged image. Scale bars represent 10µm.
(F-G) Bar graphs indicate the average number of MIG-14::GFP positive puncta, and MIG-14::GFP fluorescence intensity. The number of MIG-14::GFP positive puncta is significantly decreased in animals treated with RNAi against *bec-1* and similarly in *vps-34 RNAi.* The fluorescence intensity of MIG-14::GFP increased in animals treated with RNAi against *bec-1* or *vps-34* Asterisks indicate a significant difference in the on-tailed Student's *t*-test (** P< 0.005, *** P<0.0005, n.s.: not significant).

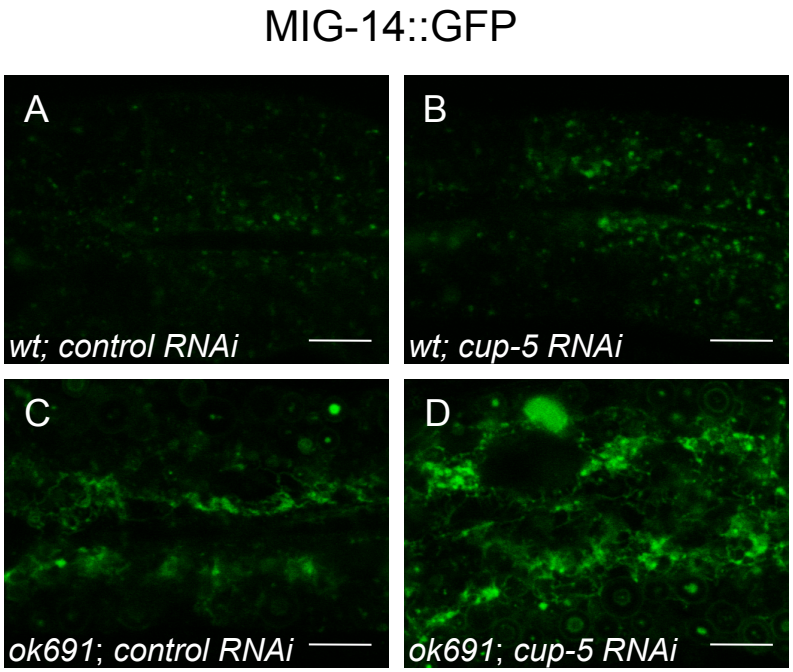

Fig. 4S: RNAi to the lysosomal biogenesis *cup-5* increases MIG-14::GFP to nearly wild-type levels in the *bec-1* mutant animals. Representative images of animals that are wild-type (A,B) or bec-1(ok691) mutant (C,D). Animals were treated with control RNAi (A,C) or the lysosomal biogenesis gene *cup-5 (REF).* Treatment with *cup-5* restores the levels of MIG-14::GFP in *bec-1* mutants to that of wild-type animals. Scale bars represent 10μm. The quantification for this experiment is on Fig. 3J.

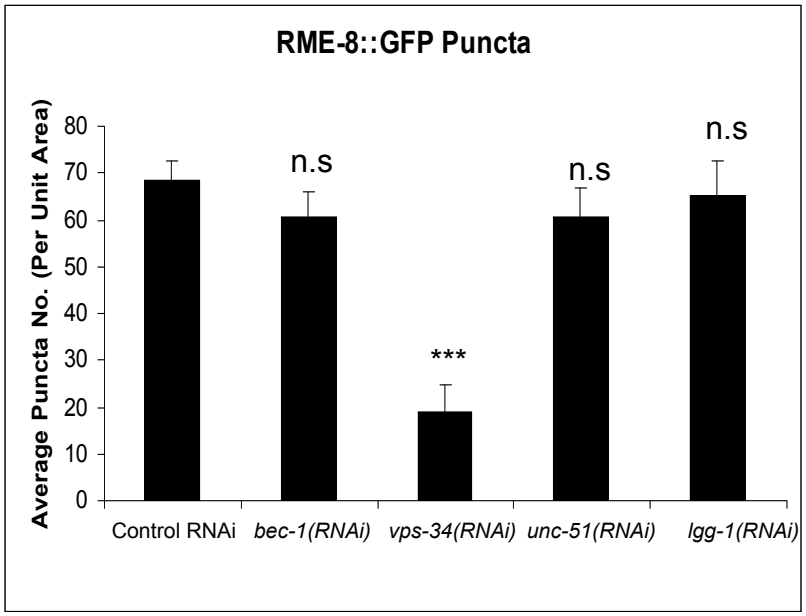

Fig. 5S: RNAi against *vps-34* decreases the number of RME-8::GFP positive puncta. Bar graphs indicate the average number of RME-8::GFP positive puncta. The number of RME-8::GFP positive puncta is significantly decreased in animals treated with RNAi against *vps-34,* but not affected in animals treated with RNAi against bec-1. However, a decrease in *RME-8::GFP was observed in bec-1(ok691)* and shown in Fig. 3I. We observed no effect in the number of RME-8 positive puncta in animals that were treated with RNAi against the autophagy genes *unc-51/ATG1* or *lgg-1.* Asterisks indicate a significant difference in the on-tailed Student's *t*-test (*** P<0.0005, n.s.: not significant).

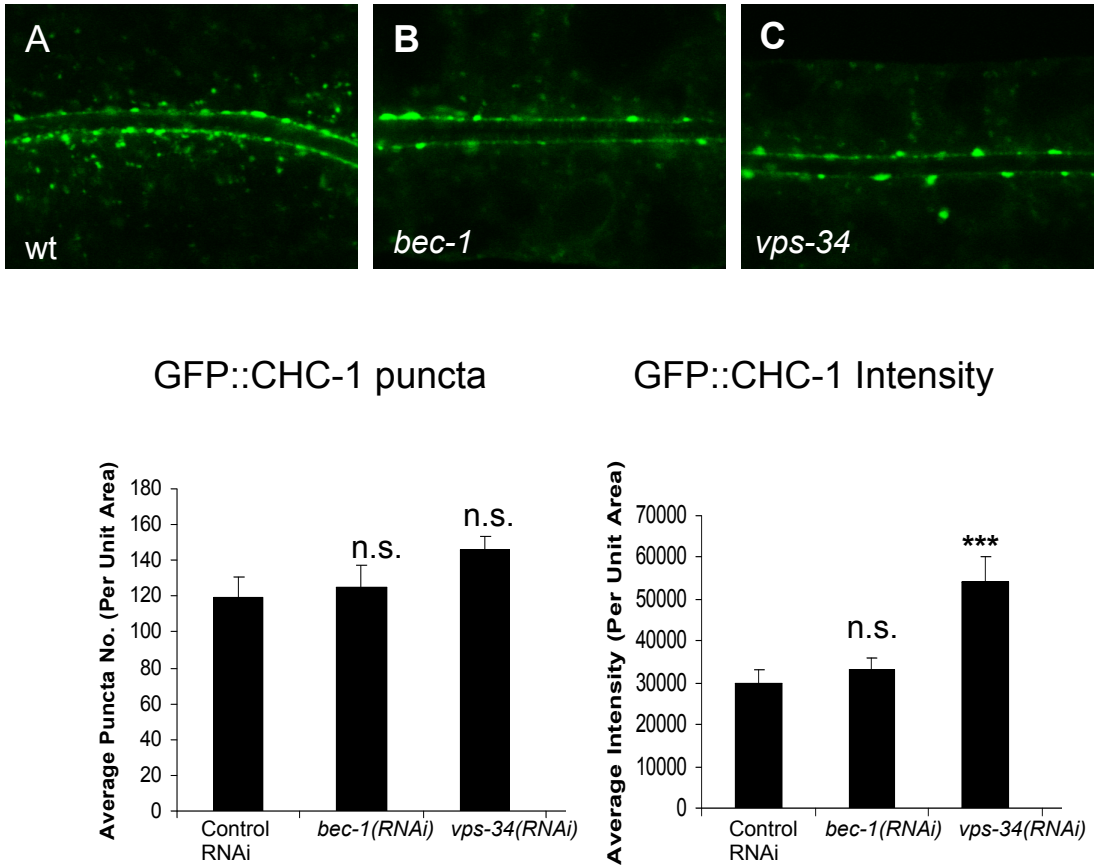

Fig. 6S: The number of clathrin GFP::CHC-1 positive endosomes is not affected in animals treated with RNAi against *bec-1* or *vps-34*. A significant increase in the intensity of GFP::CHC-1 was noted in animals that have treated with RNAi against *vps-34,* suggesting that clathrin accumulates in animals lacking *vps-34*. Asterisks indicate a significant difference in the on-tailed Student's *t*-test (*** P<0.0005, n.s.: not significant).

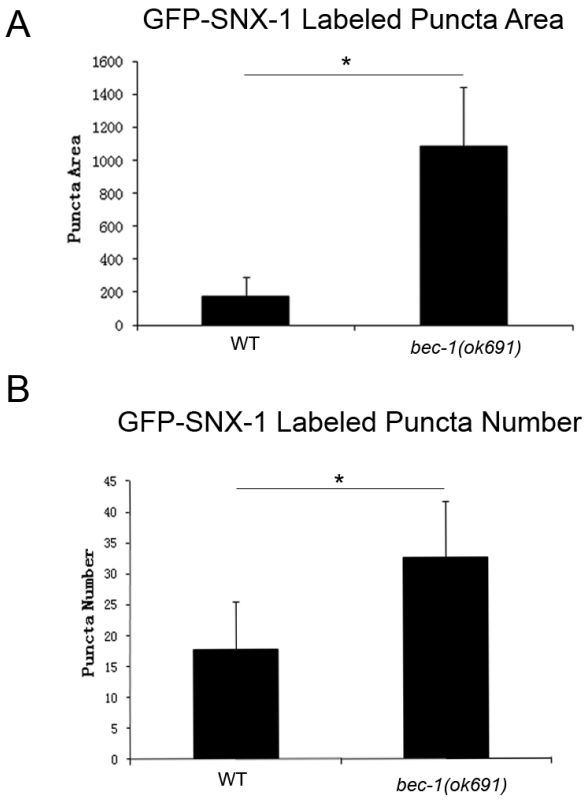

Fig. 7S: *bec-1* loss of function increases the number and the size of GFP::SNX-1 positive puncta. Bar graphs indicate the average area of GFP::SNX-1 labeled puncta (A) and the number of GFP::SNX-1 positive puncta. The number of SNX-1:GFP positive puncta is significantly increased in *bec-1(ok691)* animals. A similar phenotype has been reported for *rme-8(b1023)* mutants (Shi et al., 2009). Representative images of this

quantification are shown in Fig. 3G. Asterisks indicate significant difference in the on-tailed Student's *t*-test (* $P<0.05$).